Blood Contrast Agents Enhance Intrinsic Signals in the Retina: Evidence for an Underlying Blood Volume Component

Jesse Schallek and Daniel Ts'o

Purpose. To examine the extent to which neurovascular coupling contributes to stimulus-evoked intrinsic signals in the retina.

Methods. The retinas of five adult cats were examined in vivo. Animals were anesthetized and paralyzed for imaging stability. The retinas were imaged through a modified fundus camera capable of presenting patterned visual stimuli simultaneous with a diffuse near infrared (NIR).

Results. Injections of nigrosin increased signal strength by as much as 36.3%, and indocyanine green (ICG) increased signal magnitudes by as much as 38.1%. In both cases, intrinsic signals maintained a colocalized pattern of activation corresponding to the visual stimulus presented. The time course of the evoked signals remained unaltered. The spectral dependency of signal enhancement mirrored the absorption spectra of the injected dyes.

Conclusions. The data are consistent with a neurovascular coupling effect in the retina. Patterned visual stimuli evoke colocalized NIR reflectance changes. The patterned decrease in reflectance was enhanced after nigrosin or ICG was injected into the systemic circulation. These findings suggest stimulus-evoked changes in blood volume underlie a component of the retinal intrinsic signals. (*Invest Ophthalmol Vis Sci.* 2011;52:1325–1335) DOI:10.1167/iovs.10-5215

Optical signals intrinsic to the vertebrate retina that are evoked by visual stimulation have been observed using a variety of techniques including reflectance measurements under flood illumination[1–10] and, more recently, advanced imaging techniques such as adaptive optics scanning laser ophthalmoscopy (AOSLO)[11] and functional optical coherence tomography (fOCT)[12–14] (Suzuki W, et al. *IOVS*. 2010; 51:ARVO E-Abstract 1034). It is likely that many of these optical signals are distinct; for some, information is available regarding the underlying cellular or anatomic origins and the biophysical mechanisms responsible.

In our own studies, we have described optical imaging of changes in retinal reflectance due to patterned stimuli in the vertebrate retina in vivo (Ts'o DY, et al. *IOVS*. 2003;44:ARVO E-Abstract 2709). The signals reported in these studies are optical reflectance changes in the near-infrared range (NIR). They are thought to be different from those in the visible range, which show reflectance changes from photopigment bleaching in the photoreceptors.[15,16] The in vivo NIR signals show the strongest activations colocalized with the stimulated region of retina, suggesting a local mechanism of action that leads to a decrease in optical reflection. The biophysical origins of these signals have yet to be fully elucidated.

One plausible origin of these signals in the retina may arise from hemodynamic coupling associated with neural modulation. This neurovascular coupling has been observed in many areas of the central nervous system and forms the fundamental basis of imaging techniques such as functional magnetic resonance imaging (fMRI)[17] and intrinsic signal optical imaging in the neocortex.[18] Indeed, specific to studies of the cortex, evidence supports the concept that blood volume changes represent a component of the measured signal.[19–22]

In relation to the retina, studies primarily using laser Doppler flowmetry (LDF) have shown modulations of blood flow, velocity, and volume in response to visual stimulation.[23,24] These demonstrations have confirmed the neurovascular coupling hypothesis in the retina. What remains to be elucidated, however, is the extent to which changes in blood volume contribute to the spatially evoked NIR reflectance changes in the retina. Several reports have provided suggestive evidence that hemodynamics may be a biophysical origin of the retinal signals.[4,5,9,25] Our recent efforts have sought to expand this line of research to better understand intricate stimulus-response mechanisms of the retina considering signals may arise directly from events as early as phototransduction through the systemic retinal response.

In this study, we test the hypothesis that a component of the retinal intrinsic signals arises from blood volume changes in response to visual stimulation. Using a modified fundus camera described in previous reports,[3–5] we examined signal characteristics before and after the injection of blood contrast agents. To enhance functional blood contrast, we made systemic injections of nigrosin (India ink), which has been used to confirm effects of a blood volume component in the neocortex.[20] Alternatively, we injected indocyanine green (ICG), a dye used clinically to observe the choroidal circulation,[26,27] to act as a separate plasma-bound optical contrast agent. Here we present data demonstrating that injections of these agents effectively increased functional signal strength. The enhanced signal suggests that changes in blood volume in response to visual stimulation represent a component of the intrinsic optical signals reported in vivo.

Methods

Animals and Preparation

Five healthy adult cats between 1.5 and 5 years of age were imaged in this study. Cats were anesthetized with ketamine hydrochloride (10 mg/kg intramuscularly) and acepromazine (0.01 mg/kg) for initial

From the Department of Neurosurgery, Upstate Medical University, Syracuse, New York.

Supported by National Institutes of Health Grant EB002843/1035464.

Submitted for publication January 15, 2010; revised July 15 and September 14, 2010; accepted September 19, 2010.

Disclosure: **J. Schallek**, None; **D. Ts'o**, P

Corresponding author: Jesse Schallek, Institute for Human Performance, Room 4117, 750 East Adams Street, Syracuse, NY 13210; schallej@upstate.edu.

anesthetic. Animals were endotracheally intubated, and three intravenous (IV) lines were placed for continuous infusion of paralytic, anesthetic, and blood contrast agent infusion. Anesthetized animals were positioned in a stereotaxic frame. A sodium thiopental infusion (1–2 mg/kg/h) maintained anesthesia throughout the duration of the experiment. Animals were paralyzed with vecuronium bromide (0.1 mg/kg/h) to optimize imaging stability and minimize eye movements. Cats were artificially ventilated with room air to compensate for diaphragm paralysis. Electrocardiogram, temperature, and expired CO_2 were monitored throughout the experiment to ensure animal vitality and sufficient anesthetic and paralytic rates.

Neosynephrine (10%) and atropine (1%) were applied to the cornea at the beginning of the experiment to dilate the pupil and prevent accommodation. Low-power, 34.0-D lenses were placed on the corneas to prevent drying. The corrective power of the system was adjusted with the internal optics of the fundus camera to optimize focus of the retinal surface. The investigation adhered to the ARVO Statement for the Use of Animals in Ophthalmic and Vision Research. Animals were cared for in accordance with the Animal Welfare Act and the Guide for the Care and Use of Laboratory Animals.

Imaging

A detailed description of the imaging apparatus, stimulus presentation, and image analysis has been described in a previous report.[4] Briefly, we modified a fundus camera (Topcon, Tokyo, Japan) to project patterned 540-nm visual stimuli into the subject's eye while diffusely illuminating the fundus with NIR light. The patterned stimuli consisted of a set of vertical and horizontal bars (Fig. 1). The luminance of the visual stimuli was 7 cd/m^2. The stimuli had Michelson contrast level of more than 96% relative to background intensities. The illumination light was filtered with 10-nm-wide band-pass filters (full width, half height) ranging between 700 and 900 nm, largely outside the visible range. The NIR light was on continuously and allowed sufficient illumination of the ocular fundus while leaving the retina in the dark-adapted state. The fundus reflection of the NIR light was collected with a charge-coupled device (CCD) camera (Photometrics, Ltd., Tucson, AZ). The field of view for all images was 35°, centered within 0° to 30° of the area centralis. Image acquisition entailed collection of 2 seconds of prestimulus baseline, 3 seconds of stimulus, and 5 seconds of poststimulus recovery at a rate of 2 Hz. At least 12 seconds were allowed between stimulus presentations to allow for adequate signal recovery. Stimuli were presented to the retina in a randomized fashion, and two to four stimulus-evoked acquisitions of the same stimulus type were averaged to increase the signal-to-noise ratio. Image acquisition was synchronized to respiration and heartbeat to reduce experimental variability and allow for removal of related biological artifacts.

Injected Agents

Nigrosin, (acid black 2; Sigma-Aldrich, St. Louis, MO) was dissolved in sterile saline (0.9% NaCl) for 3 hours or less before injection. Dosage was calculated to deliver 33 to 34 mg/kg body weight. The nigrosin solute was diluted down into 20 mL sterile saline, and the solution was passed through a 22-μm pore sized filter before injection. The filtered solution was injected into the cat's saphenous vein through a motorized syringe pump. The rate of infusion was between 20 and 40 mL/h (the typical duration was 20–30 minutes for the entire bolus). During the injection, the subject's heart rate, temperature, and CO_2 volume were carefully monitored for signs of distress. On completion of the nigrosin experiments, animals were humanely euthanatized at the completion of the imaging session by a lethal overdose of sodium thiopental (Pentothal, (100 mg/kg IV; Abbott Laboratories, North Chicago, IL). Two cats received nigrosin injections.

ICG (cardiogreen; Sigma-Aldrich) was diluted into sterile saline (0.9% NaCl) to create a final concentration of 1.0 to 1.5 mg/mL. The solution was filtered through a 22-μm pore filter. ICG solution was made fresh 1 hour before injection, and the solution was kept in the dark to minimize the degradation kinetics of the solution.[28] The drug was delivered through the saphenous vein in the hind limb of

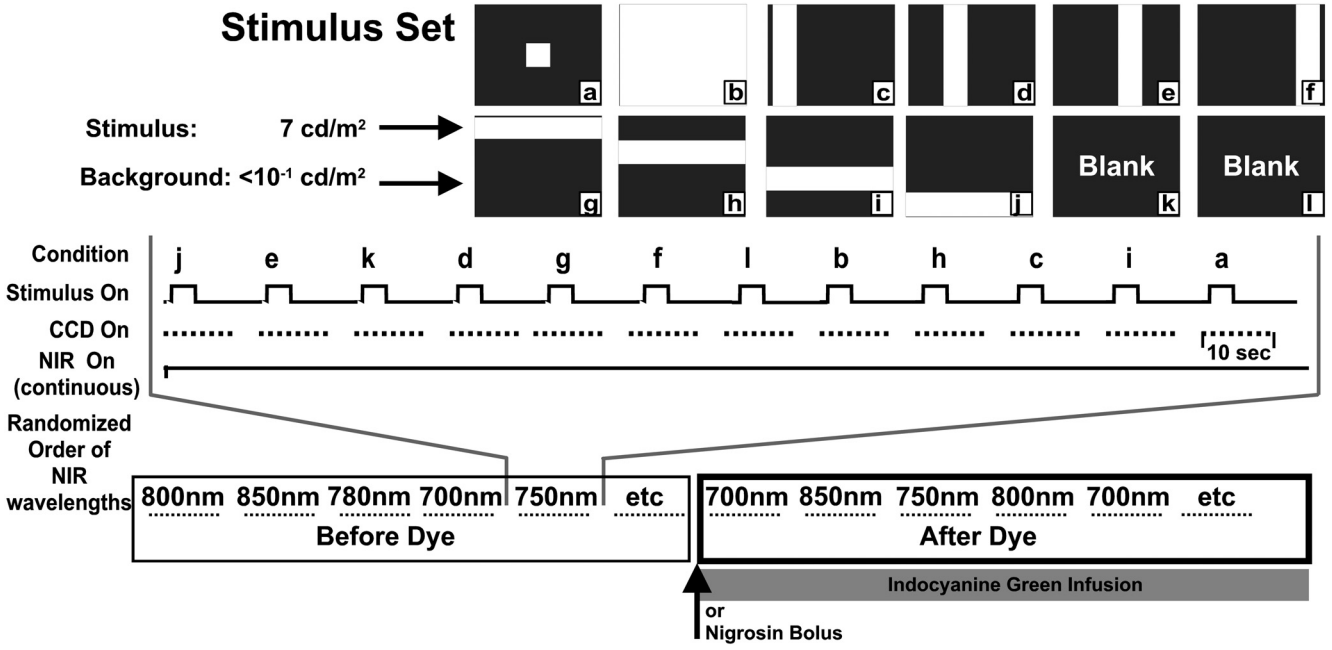

Figure 1. Imaging and experimental paradigm. *Top*: the full stimulus set used to evoke the intrinsic signal response. Patterned visual stimuli (540 ± 30 nm) were 7 cd/m^2 measured at the cornea. Background light levels were <0.1 cd/m^2. (**a–l**) Stimulus conditions 1 to 12 were presented in a randomized block trial format. *Middle*: the CCD camera captured 10 seconds of data at 2 Hz. At least 12 seconds were allowed between stimulus presentations to enable sufficient time for signal recovery. NIR illumination was on continuously throughout the block trial format. Four to eight blocks of this format were averaged to improve the signal-to-noise ratio. This block format was repeated under different illumination wavelengths centered at wavelengths 700, 750, 780, 800, 850, and 900 nm (passband = 10-nm wide, full-width at half-height). Order of illumination wavelengths was randomized in each experiment. *Bottom*: a continuous infusion of ICG or a single bolus of nigrosin was given approximately halfway through the experiment. The same stimulus conditions and wavelengths were imaged again in the post-dye condition.

the subject. An initial bolus of 1.5 mg/kg body weight was given to initialize the systemic concentration. Immediately after, a slow infusion of the drug was administered through a motorized syringe pump to counteract the effects of the fast hepatobiliary clearance rate of the dye in the cat.[29] Infusion rate was set to deliver 190 to 380 μg/kg/min over the course of 3 to 4 hours. Animals receiving ICG were allowed to recover for 5 weeks before the next imaging experiment.

Statistical Analysis

Analysis techniques are described in more detail in a previous report.[4] Fractional change in reflectance was calculated over regions of interest (ROIs) for several stimulus conditions that demonstrated clear patterned representations of stimulus-evoked activity. The fractional change in reflectance (dR/R) was calculated as follows:

$$\text{Region of interest } dR/R_{(n)} = \frac{(ROI_n - ROI_o)}{ROI_o} \quad (1)$$

where R is the reflection intensity value of the camera readout, and dR is the change in value from the reference, unstimulated frame. The ROI is a user-selected 11 × 11–pixel region of interest in the image held constant for each $frame_{(n)}$. ROI_o measures the baseline reflectance for the specified region of interest. The 11 × 11–pixel ROIs correspond to a 1.5° to 1.9° field of view in the retina. The ROIs were centered over areas showing typical patterned activations as seen in previous reports.[3–5]

After dye injections, the baseline reflectance state became darker because of the dye absorption (Fig. 2). Therefore, a new post-dye baseline (unstimulated frame) was established after injection had reached steady state values. This new reference was taken to be the first frame of each 20 frames of acquisition. This technique also compensated for slow "DC" drifts in retinal reflectance over the course of hours. To ensure consistency, the imaged field of view and ROI coordinates were identical before and after blood contrast agents were injected. This was confirmed by registration of landmarks in the surface vessel map.

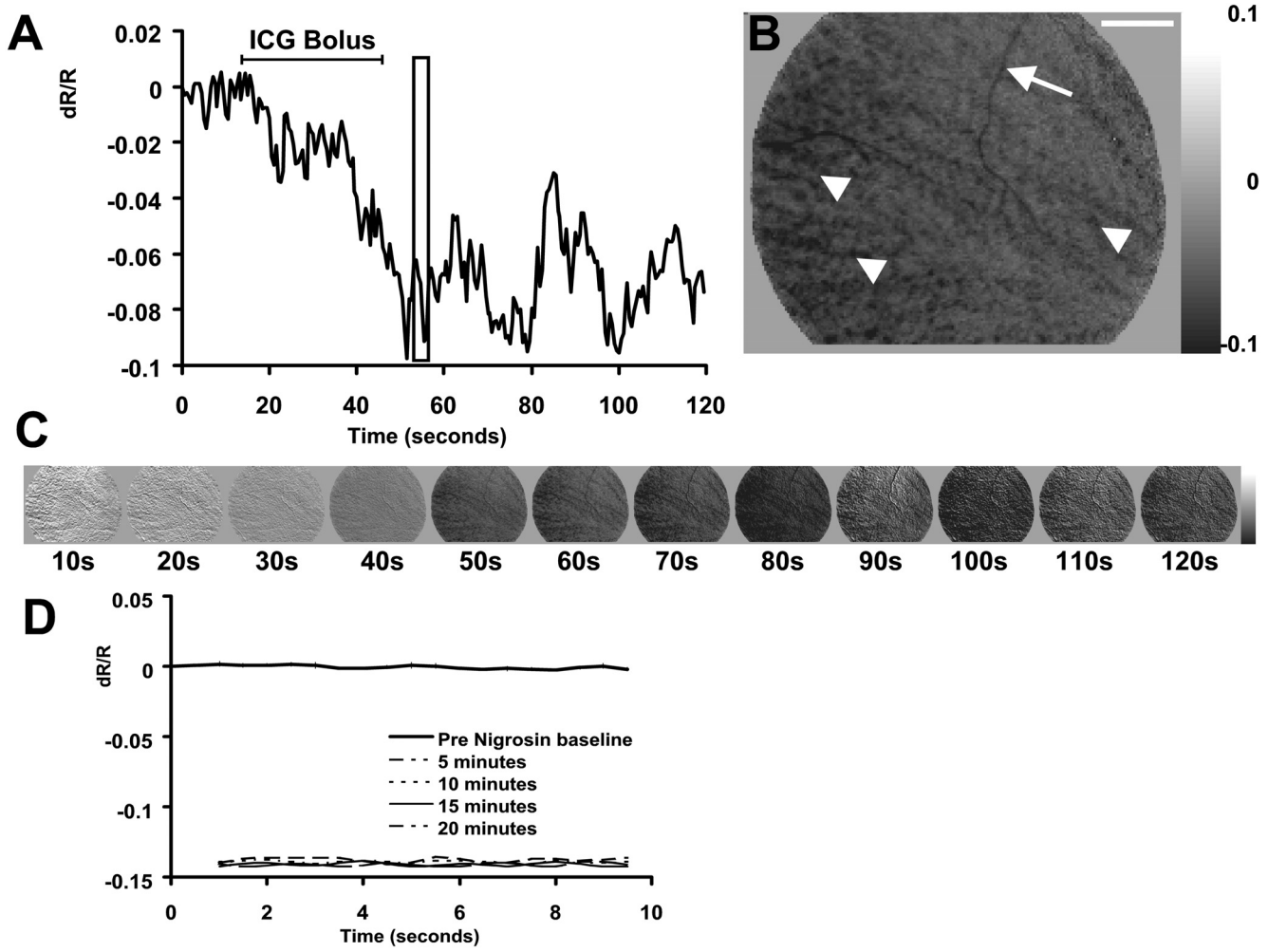

Figure 2. Retinal reflectance decrease reveals successful contrast agent infusion. (**A**) The time course of retinal reflectance after a single ICG bolus injection. Data show the reflectance of a 7° × 7° ROI after the systemic injection of 11 mg ICG (7.3 mL). The overall retinal reflectance became darker by upward of 9%. (**B**) Snapshot of the retinal image from the boxed region at 55 seconds. The overall retinal image decreases in reflectance. Pixels in this image dominate the darker end of the grayscale map (*right*). Additionally, several features in the image become recognizably darker. *Arrow*: superficial vessels darken because of the increased absorption of ICG within the blood circulation. *Arrowheads*: striated pattern indicative of the deeper choroidal circulation. Scale bar in upper right represents 6°. (**C**) Imaged sequence of the data in (**A**) at 1/20th the temporal resolution. The grayscale limits of each image have been locked at ±0.1 dR/R to demonstrate that the entire reflectance of the fundus becomes darker. (**D**) Reflectance changes from nigrosin injection. Ten seconds of data were collected without the presentation of a stimulus before injection (*bold trace*; values near zero). Retinal reflectance was measured in reference to the preinjection condition at 5, 10, 15, and 20 minutes after a bolus injection of nigrosin. Data from 5 to 20 minutes after the injection show the consistency of the change in reflectance, establishing a new solid baseline.

Unless otherwise noted, data are presented as averaged ROI response (fractional reflectance, dR/R) across all experiments before and after contrast injection. Signal magnitude was calculated as the maximum signal deflection in the peristimulus through poststimulus acquisition period ($t = 0$–8 seconds from stimulus onset). Because of the relatively monophasic signal development,[4] the largest signal was observed near the point of longest stimulus integration. Therefore, in the 3-second stimulus paradigm, maximal values typically occurred between 3.0 and 4.5 seconds after stimulus onset (see Figs. 3, 4, and 6 for examples). Where appropriate, data were normalized to preinjection values. The calculated average preinjection magnitude scale factor was applied to each intrinsic signal acquisition for each animal tested. Each observation data point corresponded to an average of four data acquisitions for the same stimulus condition. Because the data were presented in a randomized block trial paradigm with sufficient time for signal recovery, we considered each observation as independent. Data were normally distributed around the mean. Thus, statistics are presented as a two-sample *t*-test design, where degrees of freedom were constrained by N-1, where N equals the smaller number of preinjection or postinjection observations (conservative method) ($^*P < 0.05$, one-tailed *t*-test).

Dye Spectral Scans

Blood specimens were acquired before and after the injection of contrast agents in several cats. Blood was acquired by a toe-stick of the contralateral foot from the injection IV. Samples were placed in chilled heparinized saline (2 U/mL in 0.9% NaCl) to prevent coagulation. Samples were analyzed with a spectrophotometer (DU530; Beckman Coulter, Fullerton, CA) in wavelength scan mode to reveal the absorption spectra of blood before and after injection. Samples were diluted down to ensure the instrument was working within the linear range of operation. All scans were blanked against a cuvette containing the heparinized saline solution. Preinjection scans were subtracted from postinjection scans after normalizing each data set to values between 900 and 1000 nm, where nigrosin, ICG, and hemoglobin each had relatively low absorption characteristics.

Results

ICG and Nigrosin Successfully Infused into Systemic Circulation

Injections of nigrosin and ICG into the systemic circulation produced a prominent decrease in the global retinal reflectance. The retina became darker by 9% to 15% of baseline reflectance levels after the infusion of either dye (Fig. 2). The effect was measured by capturing a prolonged series of images during the drug infusion, where no stimulus was applied. In the case of the ICG infusion, the camera captured a continuous sequence of 240 frames (120 seconds) during the initial ICG bolus. Figure 2A shows the retinal reflectance at 800 nm became darker over the course of 2 minutes after an initial bolus of 11 mg ICG. Figure 2A shows data from a large central ROI in the fundus image (7° × 7°). The combined absorption by ICG in both the retinal circulation and the choroidal pool decreased the reflectance of the fundus by approximately 9%. The fluctuations of retinal reflectance seen in Figure 2A are likely due to the nature of the bolus injection and the initial mixing of the dye into the systemic circulation pool. Additionally, the data were from a single acquisition run, prone to variations in heart rate and other in vivo noise sources typically averaged out over repeated experiments.

A snapshot of this image sequence, taken at 57 seconds into the acquisition, is seen in Figure 2B. Several features in the fundus image reveal the successful infusion of ICG into the circulation. The arrow (top) points to a surface vessel that becomes darker, indicating the retinal circulation contained ICG. Additionally, arrowheads show the diagonally striated pattern, indicative of the choroidal circulation. The entire fundus image becomes darker, as evidenced by the dominance of dark pixels relative to the grayscale map at right (indicating a decrease in reflectance). The global darkening of the fundus can also be visualized in the imaged sequence in Figure 2C (1/20th the temporal resolution of the data seen in Fig. 2A). All images in Figure 2C are scaled to the same grayscale levels to show that the darkening is observed across the whole retinal image and not just in specific regions. Combined, these features are evidence of the successful infusion of ICG into the retinal circulation.

Injection of nigrosin had a similar effect on the retina. The global reflectance of the retina became darker by 14% in the experiment shown (Fig. 2D). A preinjection sequence was captured and plotted in bold (data near zero). The retinal reflectance relative to this baseline is plotted at 5 to 20 minutes after nigrosin injection. A steady state had been reached 5 minutes after nigrosin injection. From 5 to 20 minutes after the initial injection, the global reflectance of the retina did not show further changes in reflectance because of the stabilization of the dye in the systemic circulation (thin dotted and solid traces).

The total reflectance change from the drug injection is 1 to 2 orders of magnitude greater than the stimulus-evoked signals we report. It is important to reiterate that the reflectance changes in Figure 2 are caused by dye infusion and are not representations of stimulus-evoked changes because no visual stimulus was presented.

Stimulus-Evoked Signals after Nigrosin Injection

Intrinsic signals increased in magnitude after the injection of nigrosin (a larger stimulus-evoked decrease in reflectance). Figure 3A shows the retinal response to a vertical bar before nigrosin injection. The images show signal responses typical of those reported in previous studies.[4,5] The left and right images are from two cats (7791 and 7785). When the same stimuli were presented 20 minutes to 3 hours after nigrosin injection (Fig. 3B), the signals persisted with spatial properties that remained specific to the stimulated area of retina. The notable change was the increased magnitude of the signal, represented by a darkening of the patterned response relative to the preinjected condition (Figs. 3A, 3B). Images before and after injection are plotted on the same grayscale intensity range to reveal the effects of nigrosin on stimulus-evoked signals. Careful attention was made to keep the imaged field the same before and after injection. An example of this can be seen in the retinal image from cat 7785, in which the registration of a surface vessel was in the same position before and after injection.

Fifteen user-defined ROIs were placed over areas demonstrating strong intrinsic signals in two cats before the nigrosin injection (a sample ROI is shown in Figs. 3A and 3B for reference). Pre-dye and post-dye injection data from each experimental session were averaged, then normalized to the average pre-injection minimum. The averaged data without normalization are shown inset (Fig. 3C). Like the pre-injection condition, stimulus-evoked signals initiate within 500 ms of stimulus presentation. The dominant variable shift is in the magnitude. The data were statistically significant at the $P < 0.05$ level (two-sample *t*-test) between 5.0 and 5.5 seconds, time points representing the greatest magnitude deflection. Error bars represent ±1 SEM. The data in Figure 3C were from measurements taken at 750 nm; a similar increase in signal strength was seen at imaging wavelengths of 700 and 780 nm.

Stimulus-Evoked Signals after ICG Injection

Similar to the results of the nigrosin injection, ICG increased the strength of the stimulus-evoked signals. The retinal re-

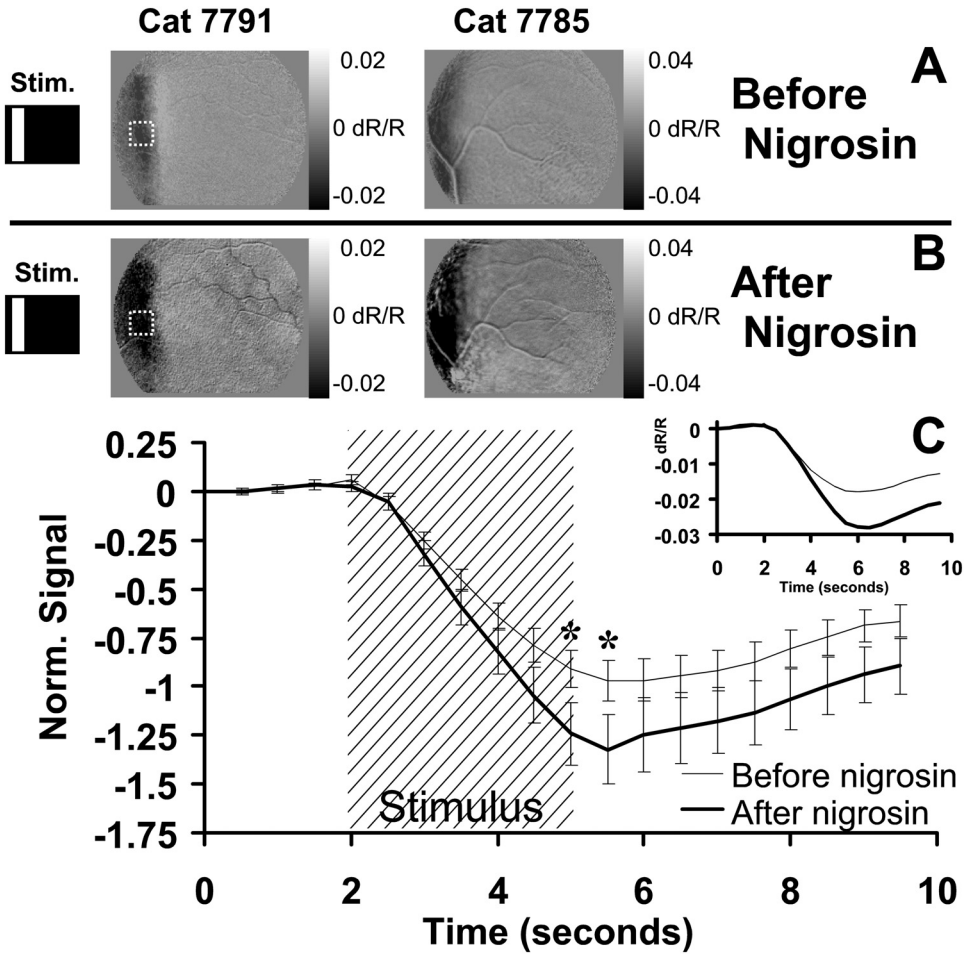

FIGURE 3. Nigrosin effect on stimulus-evoked signal. (**A**) Retinal response to a vertical bar stimulus from two cats before the injection of nigrosin. (**B**) Response to the same conditions 20 minutes after the systemic injection of nigrosin. Grayscale limits were held constant before and after injection. Signals in each cat show a darker stimulus-evoked response compared with preinjection conditions. (**C**) Fifteen ROIs were positioned over areas showing strong signal before injection. A sample ROI is demonstrated by dashed lines in Figures 2A and 2B. Preinjection values from each experiment were normalized, then averaged (*thin trace*). The same ROIs and stimulus conditions were examined after nigrosin (*bold trace*). Stimulus-evoked signals show a similar onset and decay function with an enhancement of magnitude. *Inset*: raw data magnitude before normalization. All data in Figure 2 are from imaging at 750 nm. Error bars represent ±1 SEM calculated from data on two cats. *Time points showing significance ($P < 0.05$). $n = 30$ stimulus presentations before nigrosin. $n = 39$ stimulus presentations after nigrosin.

sponses to three stimulus conditions are shown before ICG (Fig. 4A, stimulus conditions inset). The same stimulus conditions were applied during the 3 hours of constant ICG infusion. Averaged signals from the ICG infusion epoch are shown in Figure 4B. The signals during ICG infusion became visibly darker compared to the preinjection conditions measured with the same grayscale limits (±0.01 dR/R). As was seen with nigrosin injections, evoked signals remained colocalized with the stimulated region of retina. ROIs positioned over strong signal areas before the injection showed increased activations after ICG. The average responses from four experiments performed on two cats are shown in Figure 4C. Pre- and post-dye injection data from each experimental session were averaged and then normalized to the average preinjection minimum. Data before normalization can be seen (Fig. 4C, inset). ICG injections primarily modulated the amplitude of the signal but did not appreciably shift the time course of the signals. Ninety-six stimulus presentations were evaluated before ICG, and 72 conditions (same ROIs, fewer repetitions because of time constraints of ICG injection) were performed during ICG infusion. The difference in the "before" and "after" ICG conditions showed statistical significance at the $P < 0.05$ level between 3.0 and 9.0 seconds. There were more statistically significant time points in the ICG experiments (survival) than in the nigrosin experiments (terminal), possibly because of the greater number of samples collected in ICG experiments. The data in Figure 4 show the results from 780-nm illumination conditions, though a similar increase in strength was observed across all wavelengths tested (Fig. 5). Error bars show ±1 SEM.

Signal Magnitudes after Injection

For a more generalized view of the effect of blood contrast agents, data before and after blood contrast injections were compared across all wavelengths in Figure 5. The data from two successful nigrosin experiments are shown on the left. The preinjection signal strengths (abscissa) are plotted against the same conditions in the postinjection state (ordinate). Data points represent the average of 28 to 256 acquisitions captured before and again after injection. Individual points represent a single wavelength comparison (700–900 nm) before and after injection. Postinjection data were compared with preinjection data on the same experimental day, where symbols signify the date. For nigrosin experiments (left), 83.3% of data points lie above the unity line, indicating an overall increase in signal strength. Similarly, data from five ICG injection experiments on three cats also show an increase in intensity (Fig. 5, right). Here, 82.6% of the ICG data lie above the unity line. The remainder of the data points that did not demonstrate an increase in signal intensity lies on or near the unity line, indicating neither dye imposed a strong impairment on signal strength relative to the enhancement. The large amount of signal intensity spread seen in Figure 5 is due to the dependency on interrogation wavelength, where signals of greatest intensity are found at the shorter end of our tested spectrum (700–780 nm) and smaller signals are seen at the longer end of the spectrum (800–900 nm; see Figs. 6 and 7 and Schallek et al.[4]). The broad perspective of Figure 5 shows that regardless of illumination wavelength, stimulus-evoked signals became generally greater after injection of nigrosin or ICG.

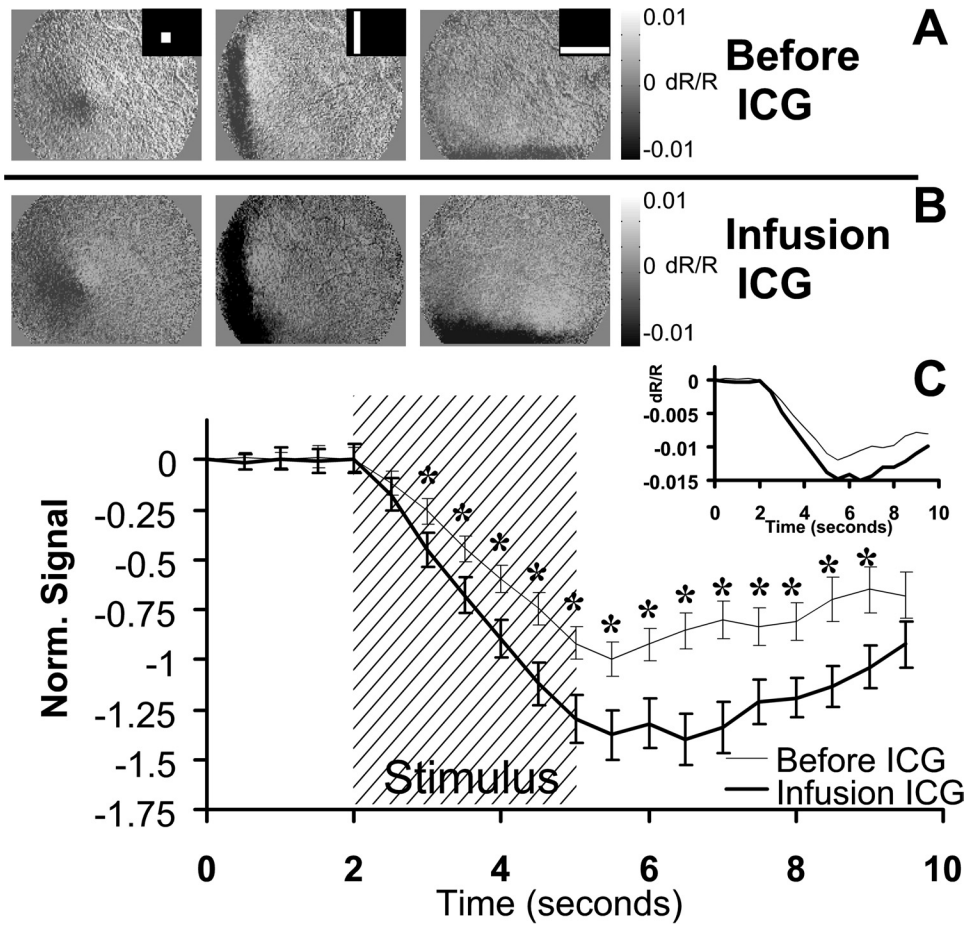

FIGURE 4. ICG effect on stimulus-evoked signal. (**A**) The retina was stimulated with patterned visual stimuli (*inset*) that evoked a patterned NIR response. (**B**) Stimulus-evoked signals became darker after the constant infusion of ICG in the systemic circulation. Grayscale levels have been locked at 0.01 to −0.01 both before and after ICG to reveal the enhanced signal strength. (**A**, **B**) Data are from an exceptional experiment on cat 7788. (**C**) Several ROIs were placed over areas displaying high signal strength before injection. *Thin trace*: the mean of the preinjection ROIs is plotted. *Bold trace*: the same ROIs were examined during the infusion of ICG. Error bars represent ±1 SEM from four experiments on two cats. Data between 3.0 and 9.0 seconds showed a significant difference ($^*P < 0.05$). $n = 96$ stimulus presentations before ICG. $n = 72$ stimulus presentations after ICG.

Signal Time Course

In each experimental set, testing ICG or nigrosin, we found that the time course of the signal remained unchanged from the preinjection condition. Similar to our previous findings,[4] we found that signals between 700 and 900 nm showed a largely monophasic growth function concurrent with retinal stimulation (Fig. 6). Normal temporal signatures with our stimulation paradigm revealed 2 seconds of prestimulus baseline reflectance, 3 to 4 seconds of signal development concurrent with stimulus duration (shaded region), and a recovery back to baseline in the poststimulus epoch (see Figs. 3, 4, 6). After injection of either agent, signal intensity was modulated most strongly during the growth phase of the signal. There was no appreciable time advance or time lag from preinjection conditions (Fig. 6, left). Signal enhancement was observed for all wavelengths with the exception of the data at 900 nm in the

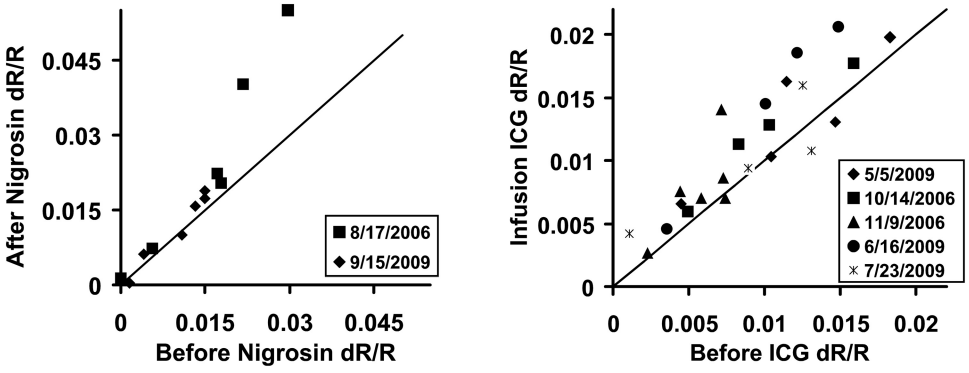

FIGURE 5. Magnitude of intrinsic signals after injection of blood contrast agents. Intrinsic signal strength is plotted before (abscissa) and after injection of contrast agents (ordinate). Each data point represents the maximum signal deflection of the experimental average for a specific wavelength (700–900 nm; see Methods). *Symbols* denote the experimental data in the legend. For nigrosin experiments (*left*), each data point represents the average of 28 to 256 acquisitions compared before and after injection. 83.3% of data lie above the unity line, indicating a general increase in signal strength. For ICG experiments, each data point represents the average of 48 to 144 acquisitions, and 82.6% of the data lie above the unity line. $n = 2$ cats for nigrosin. $n = 3$ cats for ICG.

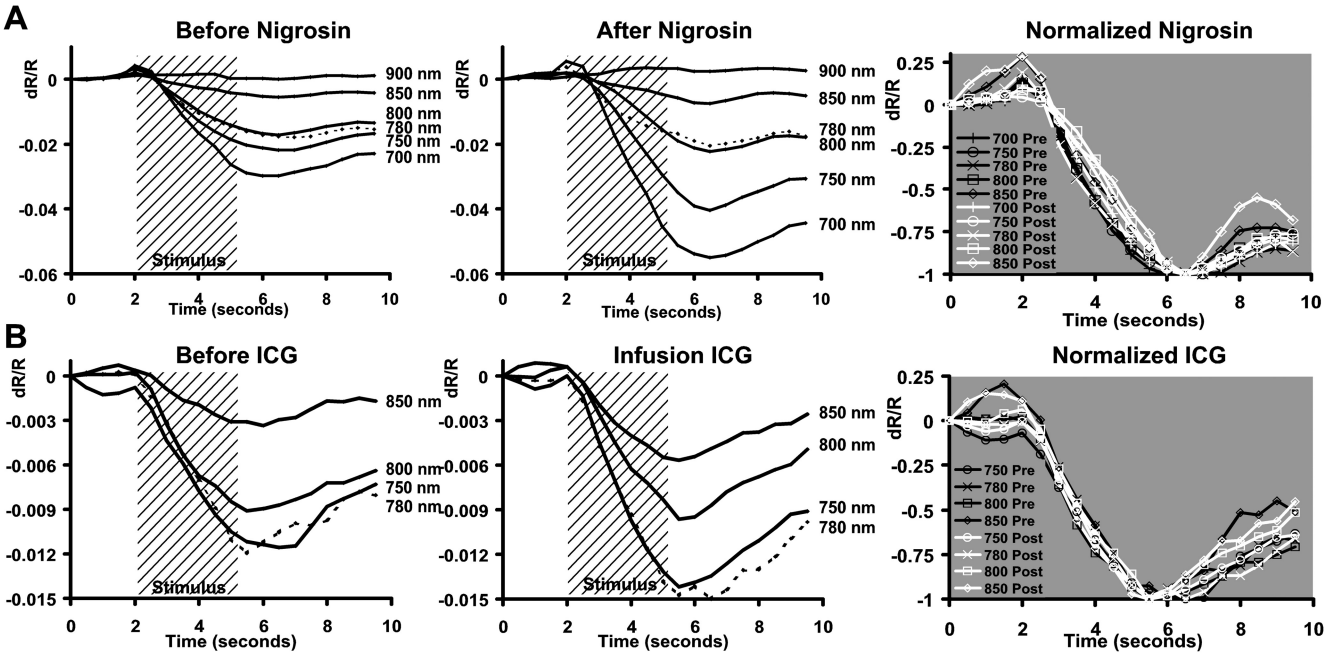

FIGURE 6. Time course of reflectance change after blood contrast injection. (**A**) Intrinsic signals plotted before and after nigrosin injection. Data are from an exceptional experiment showing the enhancement of signals as a function of interrogation wavelength. The magnitude of the signal was enhanced after injection (*middle*), especially for shorter wavelengths of 700 and 750 nm. Data from wavelengths 700 to 850 nm are normalized to the maximum deflection at right. Pre-nigrosin (*black*) and post-nigrosin (*white*) conditions show strong overlay without the development of new peaks or troughs. Temporal onset, growth, and decay functions are largely unchanged without phase advance or lag. (**B**) Time course of signals before (*left*) and during (*middle*) ICG infusion. All signals at measured wavelengths were enhanced, with notable increases at 750 and 780 nm. Pre-ICG (*black*) and post-ICG (*white*) traces retain the same onset, growth, and decay functions when normalized (*right*). (**A**, **B**, *dotted traces*) Data from 780 nm to disambiguate from surrounding traces.

nigrosin experiments (low signal-to-noise ratio). More interestingly, however, signals after nigrosin were enhanced the most in the 700- to 750-nm bands, whereas ICG injections showed the greatest enhancement in the 750- to 780-nm range, suggesting a wavelength-dependent modulation (see lower traces of middle Fig. 6).

The unchanged time course can be further appreciated in Figure 6 (right), where preinjection and postinjection conditions are normalized to the maximum deflection of the signal. Five NIR wavelengths that produced appreciable signal are shown (data from 900 nm were excluded because of insufficient signal-to-noise ratio). Signals before (black) and after (white) contrast injection show strong overlap without the development of new peaks or troughs in the time course.

Wavelength-Dependent Changes

Blood contrast injections modulated the intrinsic signals in a wavelength-dependent fashion. Consistent with previous findings,[4] we found that normal intrinsic signals were typically greatest at 700 nm and decreased in magnitude through 900 nm. After nigrosin or ICG injections, the wavelength dependence retained the same gross spectral dependency but with increased magnitude (Fig. 7A, bold lines). Subtraction of the preinjection from the postinjection state reveals the spectral shift in signal imparted by the systemic dye injection (Fig. 7B). Interestingly, the greatest modulation of signal strength occurred at different spectral regions for the two injected contrast agents. Nigrosin injections heavily increased signal magnitudes at the 700-nm end of the spectrum, whereas ICG had the greatest effect on wavelengths near ICG peak absorption (Fig. 7B). The difference spectra in Figure 6B show that injections of these dyes modulated the stimulus-evoked signal in a spectral-dependent fashion that was not a simple multiplier of the intrinsic signal source. Instead, the difference in stimulus-evoked data resembled the absorption spectra of the dye injected (Fig. 7C). A two sample *t*-test performed on matched wavelengths before and after ICG showed significance at 750, 780, and 850 nm ($^*P < 0.05$, where n = number of experiments performed on three cats). Significance was not met under nigrosin conditions, possibly because of the low sample size ($n = 2$).

Figure 7C shows the normalized absorption profiles of the injected dyes between 650 and 950 nm. The absorption profiles were calculated from blood extracted from a toe stick that compared blood absorbance before and after blood contrast injection. Both preinjection and postinjection samples showed characteristic peaks at 540 and 575 nm (data not shown), corresponding to the known absorption of hemoglobin.[22] Subtraction of preinjection absorbance from postinjection scans revealed trace amounts of the injected dye in the systemic circulation (Fig. 7C). This method of "blood subtraction" showed absorption spectra similar to samples of nigrosin and ICG in heparinized saline solution measured against heparinized saline alone (data not shown). When the differential blood scans (Fig. 7C) are compared with the change in intrinsic signal (Fig. 7B), we see the wavelengths of greatest absorption tended to modulate the stimulus-evoked signals the most.

A summary of the number of subjects and wavelengths imaged are provided in Table 1. For ICG experiments, five experiments were performed on three cats. A single experiment consisted of acquiring the stimulus-evoked response for the preinjection condition and again for the postinjection condition (Fig. 1). Data were collected under different illumination conditions (700–900 nm, where ±5 nm shows the width of the passband at half-height). An "x" represents acquisition of a pre- and post-dye injection for a specific wavelength. For ICG

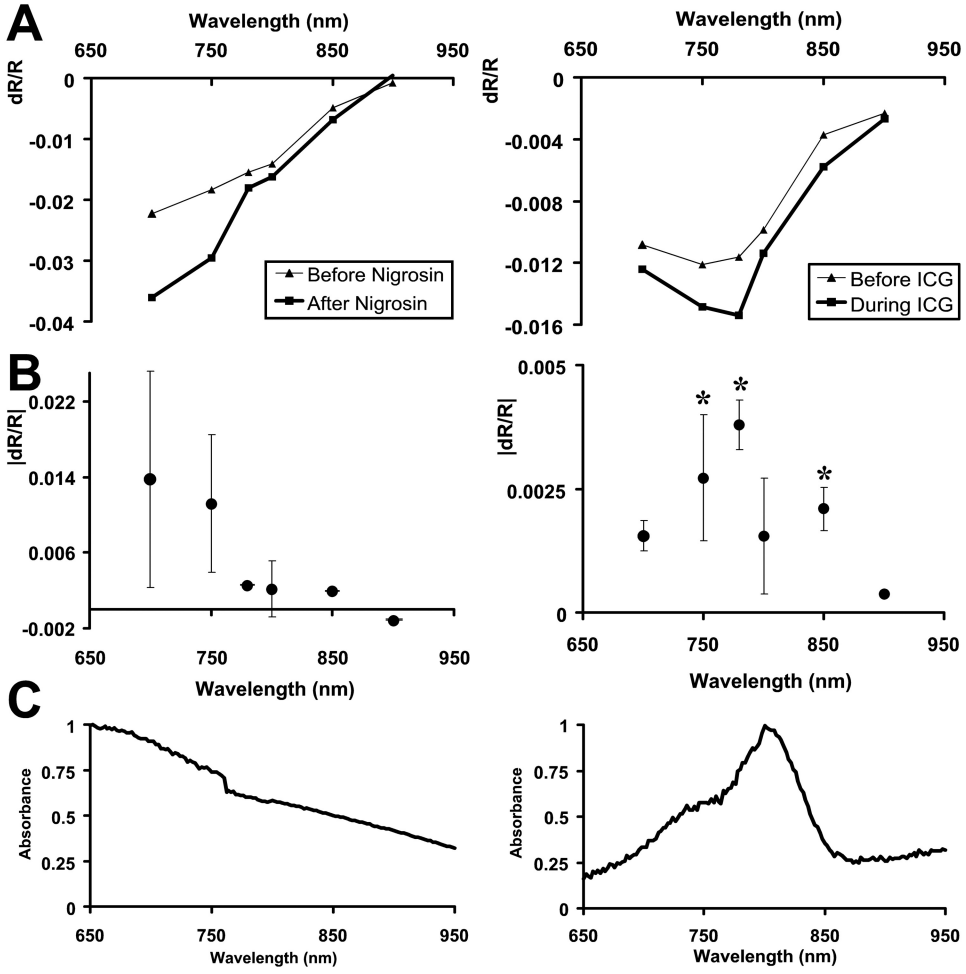

FIGURE 7. Spectral dependence of signal change after injection. (**A**) Signal strength as a function of interrogation wavelength before and after contrast agent injection. Data from all conditional experiments were averaged. *Thin traces*: preinjection conditions. *Bold traces*: after nigrosin or ICG injections, signals increased in magnitude across all wavelengths except for 900 nm. (**B**) The difference in preinjection spectra from postinjection spectra (*bold-thin traces*) reveals the spectral-dependent changes imparted by the contrast agent injection. Notably, nigrosin injections have a different spectral-dependent magnitude shift than do ICG injections. (**C**) Absorption characteristics of the injected dyes. Spectrophotometer scans of blood extracted from animals 1 hour after initial systemic injection. Blood scans after injection were subtracted from blood scans before injection to reveal the absorption spectra of the injected dye. Absorbance units were normalized to a value of 1 over the wavelengths tested in retinal scans (700–900 nm). The changes in stimulus-evoked signal strength show consistency with the absorption spectra of the injected dye.

experiments, most wavelengths tested were targeted at and around 800 nm because of the strong absorbance of ICG in that spectral region (Fig. 7C). The statistical significance of the pre- versus post-dye condition is reported as a P value (one-tailed t-test) for each wavelength. Data are reported in the same fashion for nigrosin experiments performed on two cats. Probability values did not achieve statistical significance below the $P < 0.05$ level. This might have been attributed to the low sample size ($n = 2$) of the terminal nigrosin experiments.

DISCUSSION

The purpose of this study was to further elucidate the biophysical origins of intrinsic optical signals in the retina. Specifically, the results suggest that hemodynamic changes in response to visual stimulation contribute to the reflectance signals observed. The experiments targeted the optical absorption of blood, providing more functional contrast when modulations in blood volume are present. Indeed, systemic injection of these agents increased signal strength by more than 36% after nigrosin injection and 38% after ICG infusion. This implies that the benign contrast agents are modulating the same mechanism of action despite having different optical absorption spectra. Moreover, the results did not show a decrease in signal strength. Such a finding might have raised concerns that the dyes somehow compromised the health of the retina. Instead, signals were enhanced, showing at the very least that the mechanism driving these signals was left intact. When considering ICG in particular, it is reported to be tightly bound to plasma albumin and globulins suspended in the blood plasma[30,31]; therefore, there is a low probability of extravasation and staining the surrounding retinal tissue.

When nigrosin and ICG were injected, infusion into the systemic circulation was confirmed by observing a decrease in overall retinal reflectance (Fig. 2) and by observing trace amounts of the agents in extracted blood samples (Fig. 7C). Interestingly, the retinal changes we observed after nigrosin injections (14% decrease in reflectance) were similar to those of a study using nigrosin in the neocortex that showed a 17% increase in absorption.[20] Several studies have looked at the effect of blood contrast agents on the intrinsic signals of the cortex.[18–20] Each of those studies concluded that blood volume changes underlie a component of intrinsic signals. Particularly, in the Fukuda et al.[20] study, the authors found that nigrosin injections increased the magnitude of optical signals in the cortex. Additionally, they found the postinjection time course matched the intrinsic signal time course at an isosbestic wavelength, indicating changes dominated by blood volume modulations.[20]

In relation to the signals in the retina, we found an appreciable signal at an isosbestic wavelength (800 nm). Our findings are consistent with those of a study by Crittin and Riva[25] that showed evidence of a blood volume-related signal in the optic disc and peripapillary region at 569 nm, an alternative isosbestic wavelength. The presence of an optical signal at an isosbestic wavelength implies the signal cannot be driven exclusively by the spectral contrast of oxyhemoglobin and deoxyhemoglobin.[4]

TABLE 1. Experimental Subject Data

Contrast Agent	Subject Number	NIR Wavelength 700 ± 5 nm	750 ± 5 nm	780 ± 5 nm	800 ± 5 nm	850 ± 5 nm	900 ± 5 nm
ICG	7787	x	x		x	x	
ICG	7788	x	x	x	x	x	x
ICG	7793		x	x	x	x	
ICG	7793		x	x	x	x	
ICG	7793		x	x	x	x	
	Total	2	5	4	5	5	1
	P	0.0624	0.04965	0.002415	0.12835	0.004213	NA
Nigrosin	7785	x	x	x	x	x	x
Nigrosin	7791	x	x	x	x	x	x
	Total	2	2	2	2	2	2
	P	0.3099	0.2512	0.2891	0.4037	0.1451	0.2383

For ICG experiments, cats could be imaged on multiple experimental dates because of the fast clearance rate and the low toxicity of ICG. Conversely, nigrosin experiments were terminal, which meant that pre-nigrosin versus post-nigrosin conditions could be reported only once per cat. The columns at right show the range of NIR wavelengths that were examined (center wavelength + half-width at half-height). An "x" indicates data were collected for that wavelength. Some wavelengths were not acquired in certain animals because of temporal constraints of the ICG infusion period that lasted 3 to 4 hours. All wavelengths were collected in the nigrosin experiments because temporal constraints were not an issue (terminal experiment). *P* values are reported for each wavelength tested (one tailed *t*-test, where n = number of experiments for a specific wavelength). Significant values ($P < 0.05$) are plotted as asterisks in Figure 6B. *P* value is not reported for 900 nm in the ICG condition because only one experiment was performed at that wavelength.

The proposal of a blood volume component provides one plausible explanation for the signal persistence at an isosbestic wavelength and, furthermore, for why the signal does not flip polarities at wavelengths longer than 800 nm.[4] The results show that both nigrosin and ICG modulate signal strength with the same time course as that of the normal signal at the 800-nm isosbestic wavelength (Fig. 6). In fact, all wavelengths between 700 and 900 nm in the retina show a temporal signature that appears to differ only in magnitude (Fig. 6). It is also noteworthy that the results do not show the emergence of new peaks or troughs in the time course. Taken together, the unchanged time course suggests that blood volume changes may have a dominant biophysical origin since a variety of cellular[32] and other hemodynamic origins are known to have drastically different temporal signatures.[18,22]

Regarding the change in spectral dependency, we found the modulation of signal mirrored the absorption spectra of the injected dye in Figure 7. This result is consistent with the idea that the highest blood-bound absorption provides the most functional contrast when linked to blood volume changes. Since these agents effectively increased the absorption at all our imaged wavelengths, we also saw general increases across all wavelengths (Figs. 5, 7).

Our proposal of an underlying blood volume origin complements studies using different methodologies that also show neurovascular coupling in response to visual stimulation. Riva and colleagues[24,33,34] have demonstrated through the use of LDF that the retinal circulation is sensitive to visual stimulation.[24,33,34] Flicker stimulation increased blood flow in the vessels emanating from the optic nerve head. Perceptual measures of macular blood flow using the blue-field entopic technique have also shown that visual stimulation increases flow.[35]

Most of the stimulus-evoked LDF studies report blood flow changes in the retinal circulation, the vessels that lie on the surface of the retina, whereas our technique images both the retinal circulation and the deeper choroidal circulation pool. This is because of the increased transmission of NIR light through the optically dense retinal pigment epithelium, which acts as an optical barrier for visible wavelengths. We can see evidence of the choroidal imaging capability by the striated pattern in Figure 2B and the retinal circulation, seen with the vessel contrast of the fundus images (Fig. 2B, arrow). At present, we are unable to tease apart the choroidal or retinal circulation components contributing to the NIR intrinsic signals, but it is worth mentioning that there is a notable consistency between the slow rise time of the signals we report (Figs. 3, 4, 6) and the time course of blood volume signals measured with LDF.[24] Recent reports have revealed a functional NIR signal using OCT[12–14] and AOSLO.[11] Thus far, these technologies have identified cellular origins of the intrinsic signals of the retina. Given the results of the present report, the depth resolution offered by these techniques may also provide the means to discern which circulation pool or pools contribute to a blood-volume related signal. However, it is still uncertain to what extent the fundus camera–captured signals represent the same intrinsic signals viewed with OCT (Suzuki W, et al. *IOVS.* 2010;51:ARVO E-Abstract 1034).

New advances in functional magnetic resonance imaging (fMRI) may prove to be an important tool for making comparisons and distinctions in vascular pools underlying hemodynamics in the retina. Advances in blood oxygen level-dependent (BOLD) fMRI have recently demonstrated sufficient resolution to image stimulus-driven changes in oxygen concentrations in the retina.[36] BOLD imaging is also sensitive to total hemoglobin concentration (i.e., blood volume), and detailed analyses of new fMRI data may provide information regarding the relative contributions of the retinal and choroidal circulation to stimulus-driven changes in blood volume. A comparison of all these emerging technologies will likely add to our understanding of the active mechanisms regulating stimulus-evoked hemodynamics in the retina.

An exception is that fMRI and LDF studies show dynamic stimuli tend to yield stronger signals than static stimuli.[24,36] In contrast, intrinsic signal imaging has shown that static stimuli produce indistinguishable signals from counter-flickering stimuli of equal time-averaged luminance.[4] It is likely, however, that the intrinsic signals we report are more sensitive to an outer retinal component than a ganglion cell component. This is based on the observation that the application of tetrodotoxin and other inner retinal blocking drugs has little effect on signal strength.[5] This perhaps leads to an unreconciled finding if it is presumed the signals originate from hemodynamics responding to photoreceptor activity. The current dogma of photoreceptor metabolism (especially that of rods, which dominate

throughout the cat retina[37]) is that it is highest in dark-adapted and lowest in light-adapted states.[38–40] If blood volume responds to photoreceptor metabolic demand, it might be expected that blood volume would decrease in response to a luminance increment. Yet the averaged intrinsic signals observed in the present study suggest more blood flow in response to stimulation. This experimental finding may be reconciled considering reports of increased choroidal blood flow in response to light state.[41] The results (from a human study) provide a description of a mechanism by which stimulus-evoked increases in blood volume can be observed in response to a luminance step, as is seen with our paradigm. It is also worth considering that the suppressed inner retina studies[5] might have left the active vasodilation mechanism linked to the inner retina metabolism intact. This hypothesis requires a more detailed investigation and may provide important evidence, helping to unravel the active mechanisms of neurovascular coupling in the retina.

The results of this study highlight a hemodynamic origin that is absent in similar studies performed in vitro.[2] Establishing the presence of a neurovascular component provides for a more complete understanding of the signal origins in an emerging field of noninvasive functional imaging of the retina. In particular, the close colocalization of the stimulus-response characteristics[1,4,5,10,11] suggests there exists a local mechanism for the observed response. If indeed hemodynamics are the dominant biophysical origin of the signals, these findings instill a greater appreciation for the neurovascular coupling specificity in the retina. Intrinsic signal imaging may be well suited to complement existing techniques, if not fill a new niche for functional assessment of the retina in vivo.

In conclusion, we have demonstrated that systemic injections of blood contrast agents increase stimulus-evoked reflectance signals. Signals remain spatially colocalized to the stimulated region of the retina with a time course that is not appreciably shifted. Additionally, the change in spectral dependence of the stimulus-evoked signal mirrored the absorption spectra of the contrast agent that was injected. Collectively, these findings add further support to the hypothesis that visual stimulus-evoked blood flow modulations underlie a component of intrinsic signals of the retina.

References

1. Abramoff MD, Kwon YH, Ts'o D, et al. Visual stimulus-induced changes in human near-infrared fundus reflectance. *Invest Ophthalmol Vis Sci*. 2006;47:715–721.
2. Yao XC, George JS. Dynamic neuroimaging of retinal light responses using fast intrinsic optical signals. *Neuroimage.* 2006;33:898–906.
3. Ts'o D, Schallek J, Kwon Y, Kardon R, Abramoff M, Soliz P. Noninvasive functional imaging of the retina reveals outer retinal and hemodynamic intrinsic optical signal origins. *Jpn J Ophthalmol.* 2009;53:334–344.
4. Schallek J, Li H, Kardon R, et al. Stimulus-evoked intrinsic optical signals in the retina: spatial and temporal characteristics. *Invest Ophthalmol Vis Sci.* 2009;50:4865–4872.
5. Schallek J, Kardon R, Kwon Y, Abramoff M, Soliz P, Ts'o D. Stimulus-evoked intrinsic optical signals in the retina: pharmacologic dissection reveals outer retinal origins. *Invest Ophthalmol Vis Sci*. 2009;50:4873–4880.
6. Yao XC, Zhao YB. Optical dissection of stimulus-evoked retinal activation. *Optics Express.* 2008;16:12446–12459.
7. Tsunoda K, Oguchi Y, Hanazono G, Tanifuji M. Mapping cone- and rod-induced retinal responsiveness in macaque retina by optical imaging. *Invest Ophthalmol Vis Sci.* 2004;45:3820–3826.
8. Nelson DA, Krupsky S, Pollack A, et al. Special report: noninvasive multi-parameter functional optical imaging of the eye. *Ophthal Surg Lasers Imaging.* 2005;36:57–66.
9. Hanazono G, Tsunoda K, Kazato Y, Tsubota K, Tanifuji M. Evaluating neural activity of retinal ganglion cells by flash-evoked intrinsic signal imaging in macaque retina. *Invest Ophthalmol Vis Sci.* 2008;49:4655–4663.
10. Hanazono G, Tsunoda K, Shinoda K, Tsubota K, Miyake Y, Tanifuji M. Intrinsic signal imaging in macaque retina reveals different types of flash-induced light reflectance changes of different origins. *Invest Ophthalmol Vis Sci.* 2007;48:2903–2912.
11. Grieve K, Roorda A. Intrinsic signals from human cone photoreceptors. *Invest Ophthalmol Vis Sci.* 2008;49:713–719.
12. Srinivasan VJ, Chen Y, Duker JS, Fujimoto JG. In vivo functional imaging of intrinsic scattering changes in the human retina with high-speed ultrahigh resolution OCT. *Optics Express.* 2009;17:3861–3877.
13. Tumlinson A, Hermann B, Hofer B, et al. Techniques for extraction of depth-resolved in vivo human retinal intrinsic optical signals with optical coherence tomography. *Jpn J Ophthalmol*. 2009:315–326.
14. Drexler W. Cellular and functional optical coherence tomography of the human retina: the Cogan Lecture. *Invest Ophthalmol Vis Sci.* 2007;48:5340–5351.
15. Campbell FW, Rushton WA. Measurement of the scotopic pigment in the living human eye. *J Physiol.* 1955;130:131–147.
16. Hood C, Rushton WA. The Florida retinal densitometer. *J Physiol.* 1971;217:213–229.
17. Ogawa S, Lee T, Kay A, Tank D. Brain magnetic resonance imaging with contrast dependent on blood oxygenation. *Proc Natl Acad Sci U S A.* 1990;87:9868–9872.
18. Frostig RD, Lieke EE, Ts'o DY, Grinvald A. Cortical functional architecture and local coupling between neuronal activity and the microcirculation revealed by in vivo high-resolution optical imaging of intrinsic signals. *Proc Natl Acad Sci U S A.* 1990;87:6082–6086.
19. Cannestra AF, Pouratian N, Shomer MH, Toga AW. Refractory periods observed by intrinsic signal and fluorescent dye imaging. *J Neurophysiol.* 1998;80:1522–1532.
20. Fukuda M, Rajagopalan UM, Homma R, Matsumoto M, Nishizaki M, Tanifuji M. Localization of activity-dependent changes in blood volume to submillimeter-scale functional domains in cat visual cortex. *Cereb Cortex.* 2005;15:823–833.
21. Shmuel A, Yacoub E, Pfeuffer J, et al. Sustained negative BOLD, blood flow and oxygen consumption response and its coupling to the positive response in the human brain. *Neuron.* 2002;36:1195–1210.
22. Malonek D, Grinvald A. Interactions between electrical activity and cortical microcirculation revealed by imaging spectroscopy: implications for functional brain mapping. *Science.* 1996;272:551–554.
23. Riva CE, Cranstoun SD, Petrig BL. Effect of decreased ocular perfusion pressure on blood flow and the flicker-induced flow response in the cat optic nerve head. *Microvasc Res.* 1996;52:258–269.
24. Riva CE, Harino S, Shonat RD, Petrig BL. Flicker evoked increase in optic nerve head blood flow in anesthetized cats. *Neurosci Lett.* 1991;128:291–296.
25. Crittin M, Riva CE. Functional imaging of the human papilla and peripapillary region based on flicker-induced reflectance changes. *Neurosci Lett.* 2004;360:141–144.
26. Kramer M, Mimouni K, Priel E, Yassur Y, Weinberger D. Comparison of fluorescein angiography and indocyanine green angiography for imaging of choroidal neovascularization in hemorrhagic age-related macular degeneration. *Am J Ophthalmol.* 2000;129:495–500.
27. Bischoff PM, Flower RW. Ten years experience with choroidal angiography using indocyanine green dye: a new routine examination or an epilogue? *Doc Ophthalmol.* 1985;60:235–291.
28. Saxena V, Sadoqi M, Shao J. Degradation kinetics of indocyanine green in aqueous solution. *J Pharmaceut Sci.* 2003;92:2090–2097.
29. Center SA, Bunch SE, Baldwin BH, Hornbuckle WE, Tennant BC. Comparison of sulfobromophthalein and indocyanine green clearances in the cat. *Am J Vet Res.* 1983;44:727–730.

30. Landsman ML, Kwant G, Mook GA, Zijlstra WG. Light-absorbing properties, stability, and spectral stabilization of indocyanine green. *J Appl Physiol.* 1976;40:575–583.
31. Benson RC, Kues HA. Fluorescence properties of indocyanine green as related to angiography. *Phys Med Biol.* 1978;21:159–163.
32. Cohen LB. Changes in neuron structure during action potential propagation and synaptic transmission. *Physiol Rev.* 1973;53:373–418.
33. Vo Van Toi, Riva CE. Variations of blood flow at optic nerve head induced by sinusoidal flicker stimulation in cats. *J Physiol.* 1995; 482:189–202.
34. Falsini B, Riva CE, Logean E. Flicker-evoked changes in human optic nerve blood flow: relationship with retinal neural activity. *Invest Ophthalmol Vis Sci.* 2002;43:2309–2316.
35. Scheiner A, Riva C, Kazahaya K, Petrig B. Effect of flicker on macular blood flow assessed by the blue field simulation technique. *Invest Ophthalmol Vis Sci.* 1994;35:3436–3441.
36. Duong TQ, Ngan S-C, Ugurbil K, Kim S-G. Functional magnetic resonance imaging of the retina. *Invest Ophthalmol Vis Sci*. 2002; 43:1176–1181.
37. Steinberg RH, Reid M, Lacy PL. The distribution of rods and cones in the retina of the cat (*Felis domesticus*). *J Comp Neurol.* 1973; 148:229–248.
38. Linsenmeier RA. Effects of light and darkness on oxygen distribution and consumption in the cat retina. *J Gen Physiol.* 1986;88: 521–542.
39. Stefansson E. Retinal oxygen tension is higher in light than dark. *Pediatr Res.* 1988;23:5–8.
40. Braun RD, Linsenmeier RA, Goldstick TK. Oxygen consumption in the inner and outer retina of the cat. *Invest Ophthalmol Vis Sci.* 1995;36:542–554.
41. Longo A, Geiser M, Riva CE. Subfoveal choroidal blood flow in response to light-dark exposure. *Invest Ophthalmol Vis Sci.* 2000; 41:2678–2683.